CHEMICAL ENGINEERING TRANSACTIONS
VOL. 41, 2014
A publication of AIDIC
The Italian Association of Chemical Engineering
www.aidic.it/cet
Guest Editors: Simonetta Palmas, Michele Mascia, Annalisa Vacca
Copyright © 2014, AIDIC Servizi S.r.l.,
ISBN 978-88-95608-32-7; **ISSN** 2283-9216
DOI: 10.3303/CET1441057

Hybrid Nanotubular Structures for Photoelectrocatalysis or Energy Storage Devices

Simonetta Palmas[a]*, Michele Mascia[a], Annalisa Vacca[a], Javier Llanos[b], Esperanza Mena[b], Manuel Andres Rodrigo[b], Pablo Ampudia[a]

[a]Dipartimento di Ingegneria Meccanica Chimica e dei Materiali, Università degli Studi di Cagliari. Via Marengo 2, 09123 Cagliari, Italy
[b]Chemical Engineering Department, University of Castilla-La Mancha, Edificio Enrique Costa Novella. Campus Universitario s/n, 13005 Ciudad Real, Spain
simonetta.palmas@dimcm.unica.it

The results of an experimental study devoted to the synthesis and characterisation of hybrid materials based on nanotubes (NT) of TiO_2 modified by polyaniline (PANI) are presented in this work. The results demonstrated the final material performs well when applied as photoanode for water-splitting or for energy storage devices.
TiO_2 NTs have been synthesized by anodization of Ti foils from organic solution containing fluorides. The process of electro-polymerization of aniline has been carried out by cyclic voltammetry, starting from acid aqueous solution of the monomer. The performance of the polymeric structure has been investigated under the different conditions of electropolymerisation. The electrochemical capacitance of the samples has been investigated by cyclic voltammetry (CV), electrochemical impedance spectroscopy (EIS) and galvanostatic charge–discharge tests (CDT). Moreover, photocurrent tests were performed in order to evaluate their ability in exploit the light irradiation.

1. Introduction

The combination of conducting polymers and inorganic solids is often proposed in the literature to obtain hybrid composite materials highly performing for possible applications in the field of energy storage devices. High values of capacitance can be obtained with electrochemical capacitors at which the storage of charge occurs by two mechanisms (Ambade *et al.,* 2013; Sugimoto et al., 2003): in the first one capacitance derives from charge separation at the interphase electrode/electrolyte (double layer capacitors C_{DL}), while in the second one the charge derives from more or less reversible redox processes occurring at the active surface of the electrode material (pseudocapacitors). Pseudocapacitance is produced from a bulk process whereas the double-layer capacitance is produced from a surface process (Li *et al.,* 2009). Coupling a porous matrix with high surface extension, along with an organic conductive polymer can give the right combination of properties to guarantee both the double layer and the faradic capacitive contributions to the resulting structure. When a microlayer of polymer is considered, attention should be paid on the mass of the polymer deposited (Snook *et al.,* 2007): actually, for this device architecture, making the electrodes thicker in order to store more energy is not a viable approach as thicker electrodes may suffer from electron and ion transport limitations, which reduce power density (Beidaghi and Gogotsi, 2014).
In the present work hybrid structures based on TiO_2 nanotubes modified by polyaniline (PANI) are proposed. Due to its relatively low cost, TiO_2 may represent a valid alternative to the more expensive metal oxides, such as RuO_2 which is often used to this aim (Li *et al*. 2009; Lu et al., 2012). A microlayer of PANI obtained by an in-situ electropolymerization completes the structure conferring the faradic capacitive component. Electrochemical polymerisation has a number of advantages. Particularly, there is no need for

Please cite this article as: Palmas S., Mascia M., Vacca A., Llanos J., Mena E., Rodrigo M., Ampudia P., 2014, Hybrid nanotubular structures for photoelectrocatalysis or energy storage devices, Chemical Engineering Transactions, 41, 337-342 DOI: 10.3303/CET1441057

added oxidants and electrodeposited conducting polymers are naturally integrated as a continuous uniform film on the electrode, saving the use of a binder (Peng et al., 2007).
Previous work (Palmas et al., 2014) was carried out in which PANI was electrodeposited on analogous TiO_2 support by means of galvanostatic electrolysis: in the present case cyclic voltammetry was used and different numbers of cycles were adopted in order to obtain different thickness of PANI layers.
Details are presented on the performances of samples obtained in different experimental conditions and with different PANI loads. The capacitance of the samples has been measured with different experimental techniques and the differences in the results have been discussed. Depending on the method used and on the experimental conditions adopted, different processes may be evidenced and monitored. As an example, by means of cyclic voltammetry, which is a typical technique used to derive capacitance of electrodes, over or under estimated values of capacitance may be obtained. As matter of fact, due to the large potential perturbation, the CV currents may include contributions from both localised and conduction band charge transfers, and hence give overestimated capacitance values. However, charge transfer kinetics could also affect the current according to the potential scan rate, leading to underestimated capacitance at high potential scan rates. As a steady state technique with small potential variation, electrochemical impedance spectroscopy (EIS) may be considered more reliable for measuring the capacitance with minimised effect from non-capacitive Faradic contributions (Peng et al., 2007).

2. Experimental

Titanium foils (Sigma-Aldrich®, 0.25mm thickness 99.7% metal basis) were electrochemically oxidized according to a procedure already described in previous work (Palmas et al., 2014). Briefly, after proper polishing and degreasing, oxidation was performed in glycerol / water solutions containing 0.14M NH_4F; a potential ramp (scan rate 50 mV/s) was applied from open-circuit voltage (OCV) to 20V, then the applied potential was maintained at this fixed value for two hours. A subsequent annealing treatment was needed in order to transform the amorphous phase into crystalline structure. Thermal treatment was performed in air atmosphere for 1h at 400ºC. After anodization a functionalization of the electrode surface with 4-nitrobenzenediazonium has been performed by cyclic voltammetric runs at 100 mV/s in a potential window from 0.4 to -0.7 V, in acetonitrile + 0.1 M (TBAPF6) solutions containing 2 mM of 4-nitrobenzenediazonium tetrafluoroborate. Electrochemical reduction of nitro group to amino group was performed by cyclic voltammetry in water/ethanol solution (90/10%V) containing 0.1M of KCl; the potential was varied from the open circuit potential to -1.2 V and back to 0.2 V. Scan rate was 100 mV/s. Finally, PANI polymerization was carried out on TiO_2/NH_2 electrodes. To this aim cyclic voltammetries were performed in the range from 0 to 1.4 V in aqueous solutions containing aniline (0.1M) and HNO_3 (1M). Different numbers of CV were applied in order to obtain PANI films with different thickness. In the rest of the text NT will be used to indicate a bare nanotubular structure, while modified samples will be identified with NT/PANIx, being x the number of cycles of duration of electropolymerization. The electrochemical characterization of the samples was done by cyclic voltammetry (CV), charge/discharge tests (CDT), and electrochemical impedance spectroscopy (EIS). All the runs were performed in a three electrode cell where the samples worked as anode, being a grid of platinum the counter electrode and a SCE the reference. All the values of potential given in the text refer to SCE. ZSimWin software was used to interpret the results from EIS measurements by the equivalent electrical circuit approach.

3. Results and discussion

Different techniques were adopted in order to investigate on the performance of the samples. In particular, CV, CDT, and EIS were used to derive their capacitance, and the results were discussed also interpreting the different values obtained. Actually, depending on the operative conditions at which each measurement is carried out, different capacitances may be measured at the same sample, because different phenomena may be evidenced by the different technique.
If data from cyclic voltammetry are concerned, as we expected, different results have been obtained depending on both the potential scan rate, and the potential window investigated. Figure 1a) shows an example of CV with the classical rectangular shape obtained at NT sample in a potential range in which the DL capacitive behaviour is well evident. Figure 1b) resumes the values of capacitances derived by integration of the voltammetric area at two potential scan rates, performed at NT raw sample, and after several steps of superficial modification. Lower values are generally measured at high scan rate, when superficial sites, with rapid response, are mainly responsible for the capacitve behaviour, while higher values of capacitance are obtained at low scan rate when also slow responsive sites may give their contribution to the charge storage.
No appreciable differences are noticed among the values, at least up to the PANI load is sufficiently increased.

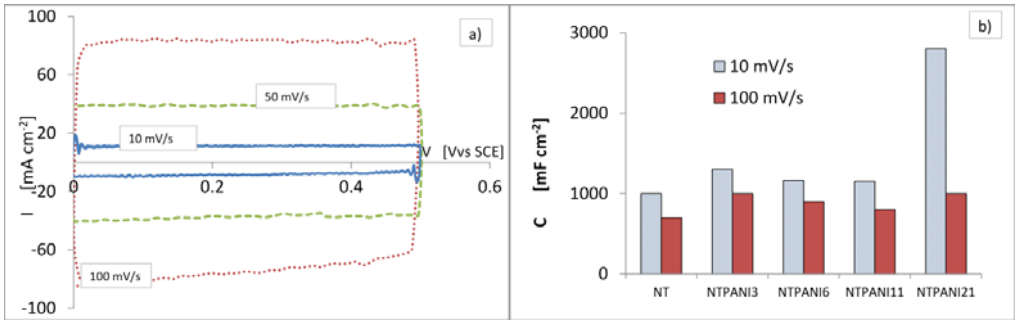

Figure 1 – a) Example of CV at NT sample performed at different scan rate; b) capacitances derived from CV runs for different samples at the lowest and highest scan rates.

On the sample with high PANI load, also a faradic contribution to the capacitance could be the responsible for the great difference between the values measured at this sample with respect to those with lower PANI loads. The strong difference between the values measured at the two scan rates at this sample could indicate that the effect of the polymer is mainly due to the bulk sites or slow response sites.
Figure 2 depicts the values of capacitance derived from CDT by the relationship:

$$C = I \cdot \frac{\Delta t}{\Delta V} = \frac{Q}{\Delta V} \qquad (1)$$

in which Q is the overall charge released (C) during the discharge period Δt carried out at a constant current density I (A/cm^2), over a potential window ΔV of 0.5V.

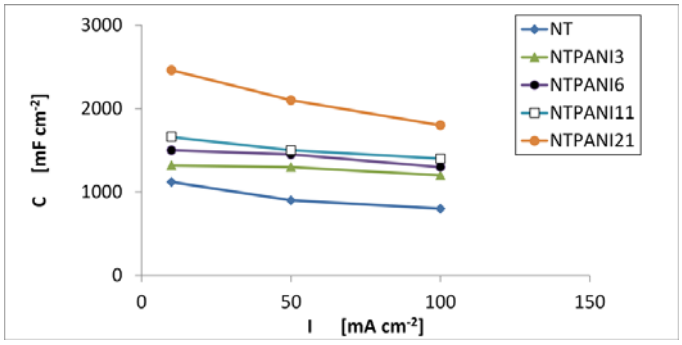

Figure 2 – Values of capacitance obtained during CDT with different discharge current, at samples with different PANI loads.

As it was expected, PANI load in the sample being the same, decreasing values of capacitance are obtained as the discharge current is increased. The values of capacitance are slightly increasing with the PANI load and, also in this case, the most important increase is obtained at the highest load.
Differences in the values obtained by CV and CDT are worth to be observed.

If data from EIS measurements are considered, different values were obtained in this case, depending on the frequency of the potential oscillation, being the highest values obtained at the lowest frequency.
Figure 3a) depicts the trend of the Nyquist plots at different PANI loads, while figure 3b) resumes the values of capacitance derived by the imaginary impedance evaluated at the minimum frequency (0.1Hz). Values of the imaginary impedance, Z", are in fact related to the so called *low frequency capacitance* C_{LF} as follows:

$$C_{LF} = \frac{1}{2\pi f Z''} \qquad (2)$$

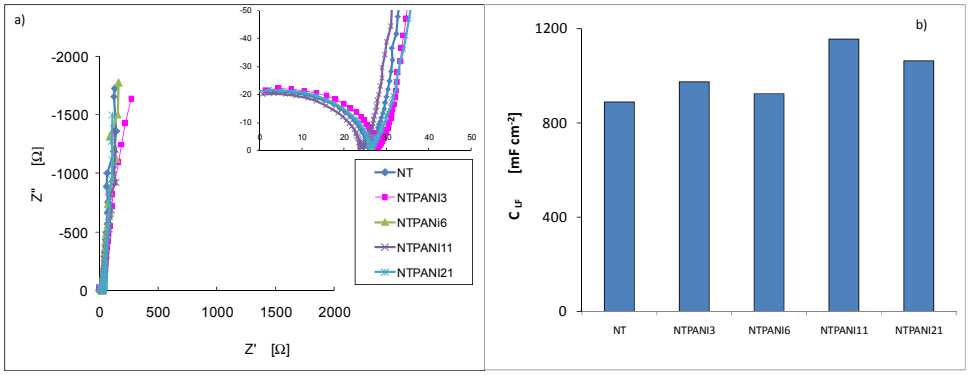

Figure 3 - Trend of the Nyquist plots at samples with different PANI loads a); values of low frequency capacitance of the related samples.

An analysis extended to the whole range of frequency, allows obtaining useful information on the different contributions of capacity. To this aim, data obtained from EIS measurements have been also analyzed with the equivalent circuit approach. Following this approach, the phenomena which occur at the electrode structure are quantitatively interpreted by means the response of an electrical circuit that, stressed with the same alternate signal, is able to give a response analogous to that of the tested sample.
Different circuits were proposed in the literature to interpret the behavior of PANI/electrodes: two or more capacitive/resistive elements were generally included in the circuit, depending on the structure. Thus for example, R(C(RC)) circuit was proposed when PANI was deposited at flat surfaces of stainless steel: two elements were considered to take account for capacity at non-homogeneous electrode surfaces and ionic diffusion process in the polymeric film (Li et al., 2009; Shinde et al., 2014). The circuit may be more complicated, when porous layers are used as support: one more RC element appeared in the circuit proposed by other authors (Xie et al., 2011, Shen et al., 2011) to fit the data obtained at PANI/TIO_2NT. According to this last paper, in the present case the electrical circuit, reported in the inset of Figure 4, allowed modelling the response obtained at raw NT and at samples with different PANI loads. Resistive contributions are included in the circuit to represent the solution resistance (R_S), the capability of the sample to charge transfer (Rct) and the resistance to leakage (R_{LK}), which can give indication about the auto-discharge of the electrode (Shen et al., 2011). In order to take account for all the contributions to the total capacitance of the electrode, a pseudocapacitance (C_{PS}) is included in the circuit along with the bulk capacitance (C_B) and double layer contribution (C_{DL}).

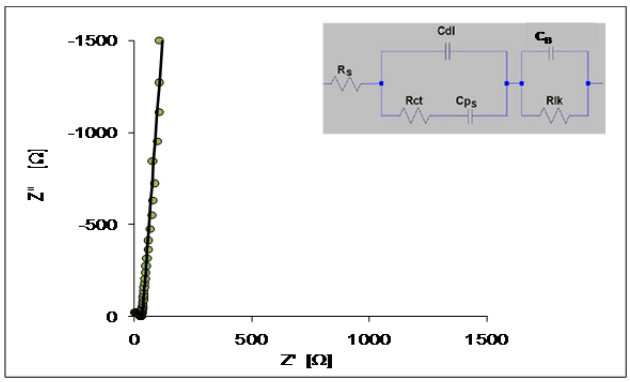

Figure 4 – Example of the Nyquist plot along with the related fit of data obtained for sample NTPANI21 by using the equivalent circuit in the inset.

Figure 4 shows an example of the fit obtained for the NTPANI21 sample: full line in the figure represents the response calculated by means of the ZSimWin software.
Figure 5 resumes a comparison between the values of the circuital parameters, derived by the fitting. In this case, data are reported as a function of the total charge, expressed in coulombs, involved during the different voltammetric cycles of PANI deposition. As it can be noticed, the extent of the C_{DL} contribution is very low, compared with that of the bulk capacitance. Actually, rather than increasing the areal extent, a

prolonged deposition of the polymer, at least up to a certain point, seems to increase the concentration of bulk sites able to interact with the solvent.
This is also confirmed by the trend of the resistances (Figure 5b): as the PANI load increases the value of R_{CT} decreases, at least up to certain values of load. Beyond this point, not only the capability of the electrode to charge exchange is affected (R_{CT} increases), but also an increase in the auto-discharge current is observed (R_{LK} decreases).

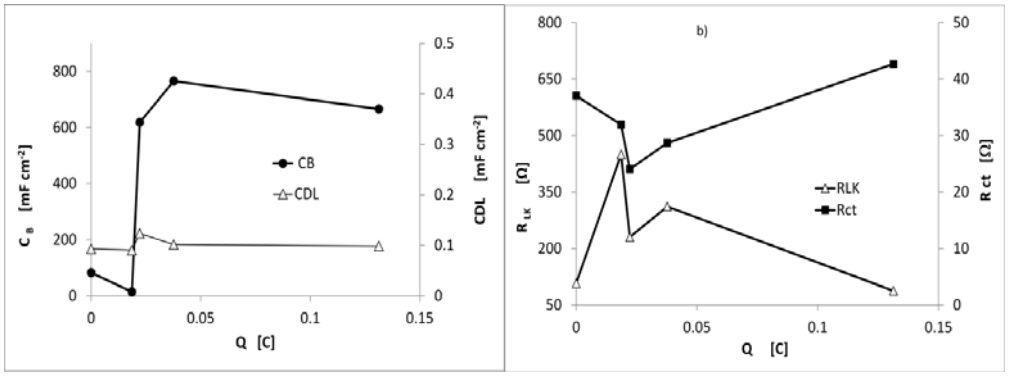

Figure 5 – Values of the circuital parameters, derived by the fitting procedure: data are reported as a function of the charge passed during the loading of PANI

Table 1 resumes the capacitances obtained at raw NT and at the samples with the maximum PANI load.
It is worth to notice the differences in the absolute values obtained from the different measurements, but also the analogies. In all the cases:

- the value measured at the PANI modified sample is higher than that measured at the raw NT sample, confirming the positive effect of the polymer
- analogous data are obtained from EIS and CV if the values at the highest scan rate are considered; this may confirm that at the lowest value of frequency (0.1Hz) examined in this work not all the active sites are involved in the process. A lower value of frequency should be needed in order to involve also the slowest sites
- the highest values obtained from charge- discharge test, which agree with those derived from CV measurements at low scan rate, may indicate that in these experiments also bulk sites are being stressed by the signal.

Table 1: Comparison between capacitance of NT and PANI21 samples. The two values derived from CV refer to capacitances calculated at the lowest and highest values of scan rate, respectively. C_B, C_{DL} and Cps represent the values of the parameters obtained by the equivalent circuit approach.

	NT C [μF/cm^2]	NTPANI21 C [μF/cm^2]
CV	1000/700	2800/1000
CDT	1120	2460
EIS C_{LF}	889	1061
C_B	82.13	666.3
C_{DL}	0.093	0.098
C_{PS}	803	383.4

The last three rows in Table 1 also report the values of the different capacitance contributions as derived from the fit of the response of the equivalent circuits. As it may be observed the sum of these values well agrees with the low frequency value C_{LF} of capacitance reported in Table 1 as derived from EIS.
Finally, the performance of the samples has been tested during the photo-electrosplitting of water, and the final data have been compared with analogous data obtained at samples in which PANI was deposited by galvanostatic electrolysis (Palmas et al., 2014). Table 2 resumes the values of photocurrents measured in KOH solution during the experiments carried out with samples irradiated by white light. In particular, the ratio I / I_{NT} between current measured at the modified sample and that measured at NT is reported in the Table 2; moreover, in order to make the comparison with previous data easier, each sample has been identified by the charge (expressed in coulombs) passed during the PANI deposition.

Table 2: Values of current ratios between photocurrent measured at modified samples with respect to that measured at NT

This work		Palmas et al., 2014	
PANI Charge [C]	Current ratio I / I_{NT}	PANI Charge [C]	Current ratio I / I_{NT}
0.022	1.6	0.036	2.0
0.038	2.0	0.072	1.6
0.131	0.39	0.144	0.19

As can be observed, the trend of data obtained at the two kinds of electrodes is similar: for both the cases a maximum of performance seems to be present at an intermediate PANI load. Accordingly with data in Figure 5, higher PANI loads become not more effective also in terms of photocurrent.

4. Conclusions

The present work was devoted to evaluate the performance of TiO_2 nanotubes, modified by polyaniline, for applications in storage devices or for water-splitting process. Different capacitances were derived from different techniques and the related values were compared and the differences among them were discussed. The electrochemical capacitance of the samples has been investigated by cyclic voltammetry (CV), electrochemical impedance spectroscopy (EIS) and galvanostatic charge–discharge tests (CDT). Moreover, photocurrent tests were performed in order to evaluate their ability in exploit the light irradiation. Results show that PANI modified TiO_2 nanotubes exhibit promising performance for photoelectrocatalysis and energy storage devices.

Acknowledgements

The authors wish to thank Andrea Sebastiano Murgia, for the support in the experimental work

References

Ambade R.B., Ambade S.B., Shrestha N.K., Nah Y.C., Han S.H, Lee W., and Lee S.H., 2013, Polythiophene infiltrated TiO2 nanotubes as high-performance supercapacitor electrodes, Chem. Commun. 49, 2308.

Beidaghi M., Gogotsi Y., 2014, Capacitive energy storage in micro-scale devices: recent advances in design and fabrication of micro-supercapacitors, Energy & Env. Sci. 7, 867-884.

Li H., Wang J., Chu Q., Wang Z., Zhang F., Wang S., 2009, Theoretical and experimental specific capacitance of polyaniline in sulfuric acid, J. of Power Sources 190, 578-586.

Lu X., Wang G., Zhai T., Yu M., Gan J., Tong Y., and Li Y., 2012, Hydrogenated TiO2 Nanotube Arrays for Supercapacitors, Nano Lett. 12, 1690−1696

Palmas S., Mascia M., Vacca A., Llanos J., Mena E., 2014, Analysis of photocurrent and capacitance at TiO2 nanotubes/polyaniline hybrid composites synthetized through electroreduction of aryldiazonium salt, RSC Advances, DOI: 10.1039/C4RA01712A

Peng C., Jin J., Chen G.Z, 2007, A comparative study on electrochemical co-deposition and capacitance of composite films of conducting polymers and carbon nanotubes, Electrochimica Acta 53, 525-537.

Shen J., Liu A., Tu Y., Foo G., Yeo C., Chan-Park M., Jiang R., Chen Y., 2011, How carboxylic groups improve the performance of single-walled carbon nanotube electrochemical capacitors?, Energy Environ. Sci. 4, 4220-4229, DOI: 10.1039/c1ee01479j.

Shinde S.S., Gund G.S., Dubal D.P., Jambure S.B., Lokhande C.D., 2014, Morphological modulation of polypyrrole thin films through oxidizing agents and their concurrent effect on supercapacitor performance, Electrochmica Acta 119, 1-10, DOI: 10.1016/j.electacta.2013.10.174.

Snook G.A., Peng C., Fray D.J., Chen G.Z., 2007, Achieving high electrode specific capacitance with materials of low mass specific capacitance: Potentiostatically grown thick micro-nanoporous PEDOT films, Electrochem. Comm., 83-88.

Sugimoto W., Iwata H., Yasunaga Y., Murakami Y., Takasu Y., 2003, Preparation of ruthenic acid nanosheets and utilization of its interlayer surface for electrochemical energy storage, Angewandte Chem. Intern. Edit. 42, 4092-4096.

Xie K., Li J., Lai Y., Zhang Z., Liu Y., Zhangc G., Huang H., 2011, Polyaniline nanowire array encapsulated in titania nanotubes as a superior electrode for supercapacitors, Nanoscale 3, 2202-2207, DOI: 10.1039/c0nr00899k.